3R optical regeneration: An all-optical solution with BER improvement

Martin Rochette, Justin L. Blows, and Benjamin J. Eggleton

Centre for Ultrahigh-bandwidth Devices for Optical Systems (CUDOS), School of Physics, University of Sydney, NSW 2006 Australia
rochette@physics.usyd.edu.au

Abstract: We demonstrate that an optical regenerator architecture providing re-amplification, re-shaping, and re-timing based on the principle of spectral shift followed by filtering can lead to bit error ratio improvement of the signal passing through it. This is in contrast with typical regenerators based on the usual principle of power conversion from a transfer function, which are unable to improve the bit error ratio. At first, we provide the theoretical basis that explains this improvement. Then we present the regenerator architecture based on spectral shift followed by filtering and provide experimental evidence of bit error ratio improvement of a noisy signal from $3x10^{-6}$ without regenerator to $2x10^{-10}$ with regenerator.

OCIS codes: (190.4360) Nonlinear optics, devices; (060.7140) Fiber optics and optical communications, ultrafast processes in fibers

Reference and links

1. P. V. Mamyshev, "All-optical data regeneration based on self-phase modulation effect," in Proc. *of 24th European Conference on Optical Communication, 1998* (IEE, UK, 1998), pp. 475-476.
2. T. Her, T. Leng, G. Raybon, J. C. Bouteiller, C. Jorgensen, K. Feder,, K. Brar, P. Steinvurzel, D. Patel, N. M. Litchinitser, P. S. Westbrook, L. E. Nelson, C. Headley, and B. J. Eggleton, "Enhanced 40 Gbit/s OTDM receiver sensitivity with all-fiber optical 2R regenerator," in *Technical Digest of the Conference on Lasers and Electro-Optics, 2002*, (Optical Society of America, Washington DC, 2002), pp. 534-535.
3. G. Raybon, Y. Su, J. Leuthold, R. J. Essiambre, T. Her, C. Joergensen, P. Steinvurzel, and K. D. K. Feder, "40 Gbit/s Pseudo-linear Transmission Over One Million Kilometers," in *Proceeding of the Optical Fiber Conference and Exhibit, 2002*, (Optical Society of America and the Laser and Electro-Optics Society, Washington DC, 2002), pp. FD10-1 - FD10-3.
4. M. Meissner, K. Sponsel, K. Cvecek, A. Benz, S. Weisser, B. Schmauss, and G. Leuchs, "3.9-dB OSNR gain by an NOLM-based 2-R regenerator," IEEE Photon. Technol. Lett. **16,** 2105-2107 (2004).
5. P. Z. Huang, A. Gray, I. Khrushchev, and I. Bennion, "10-Gb/s transmission over 100 Mm of standard fiber using 2R regeneration in an optical loop mirror," IEEE Photon. Technol. Lett. **16**, 2526-2528 (2004).
6. D. Rouvillain, F. Seguineau, L. Pierre, P. Brindel, H. Choumane, G. Aubin, J. L. Oudar, and O. Leclerc, "40 Gbit/s optical 2R regenerator based on passive saturable absorber for WDM long-haul transmission," in *Proceeding of the Optical Fiber Conference and Exhibit, 2002*, (Optical Society of America and the Laser and Electro-Optics Society, Washington DC, 2002), p. FD11-1.
7. F. Ohman, S. Bischoff, B. Tromborg, and J. Mork, "Semiconductor devices for all-optical regeneration," in *Proceedings of the 5th International Conference on Transparent Optical Networks, 2003*, (2003), pp. 41-46.
8. J. Suzuki, T. Tanemura, K. Taira, Y. Ozeki, and K. Kikuchi, "All-optical regenerator using wavelength shift induced by cross-phase modulation in highly nonlinear dispersion-shifted fiber," IEEE Photon. Technol. Lett. **17**, 423-425 (2005).
9. M. Rochette, J. N. Kutz, J. L. Blows, D. Moss, J. T. Mok, and B. J. Eggleton, "Bit error ratio improvement with 2R optical regenerators," IEEE Photon. Technol. Lett. **17**, 908-910 (2005).
10. M. Rochette, J. L. Blows, and B. J. Eggleton, "An All-Optical Regenerator that Discriminates Noise from Signal," in *Proceedings of the 31st European Conference on Optical Communication, 2005*, (IEE, UK, 2005), We2.4.1.
11. M. Rochette, L. B. Fu, V. Ta'eed, D. J. Moss, and B. J. Eggleton, " 2R Optical Regeneration: An All-Optical Solution for BER Improvement," to be published in J. Sel. Topics in Quant. Electron. **12**(6), (2006).
12. A. Papoulis, and S. U. Pillai, *Probability, random variables, and stochastic processes, 4th ed* (McGraw Hill science, New York, 2001).

#72211 - $15.00 USD Received 22 June 2006; revised 27 July 2006; accepted 27 June 2006

1. Introduction

Optical regenerators that enable signal re-amplification combined with re-shaping (2R), and even re-timing (3R) are used to limit signal degradation by noise sources in optical communication systems. For most 2R and 3R regenerators, the main regeneration mechanism is enabled from a nonlinear *power transfer function* (*f*) [1]-[8] which together with an instantaneous input power ($P_{-}(t)$) provides a deterministic output power $P_{+}(t)=f[P_{-}(t)]$, where t is time. An important characteristic of regenerators providing an output power depending only on the instantaneous input power is that they do not improve the bit error ratio (BER) of a signal passing through them [9]. That is, a noisy signal that enters such typical regenerator exits the regenerator with a BER that is worse (i.e. larger) or at best equal to the input BER. This is true for any nonlinear power transfer function or even a step-like power transfer function.

In contrast with the above comments, we recently demonstrated that a noisy signal could exit a regenerator with an improved BER, provided that the regenerator discriminates logical ones from logical zeros, by processing them with distinct power transfer functions [9]-[11]. Up to now, we found that the architecture based on the principle of spectral broadening with self phase modulation followed by filtering [1] is the only 2R architecture that could improve the BER of a noisy signal. Such regenerator represents a breakthrough because it allows a better control on the BER in amplified system when compared to standard regeneration schemes. The only limitation of this architecture arises from its 2R nature: It does not re-time the signal and therefore has no immunity against timing jitter.

In this paper, we present the first 3R regeneration architecture that leads to BER improvement. This architecture fulfils 3R regeneration and is therefore immune against timing jitter. It also displays different power transfer functions for the logical ones and logical zeros of a noisy signal, which enables BER improvement. In Section 2, we present concepts of signal and noise that will be used throughout the text. In Section 3, we present the theoretical basis that supports the concept of BER improvement by optical regenerators. In Section 4, we demonstrate that the 3R regenerator based on the principle of spectral shift and filtering has the capability to improve the BER of a noisy signal. Finally, in Section 5, we show experimental evidence of BER improvement at 40 Gb/s by this regenerator.

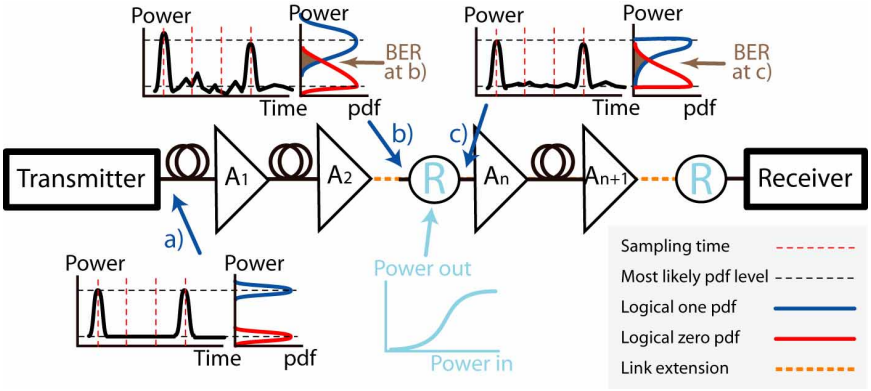

Fig. 1. Schematic of an optical communication link with typical (Class I) optical regenerators. (a) The transmitter sends a signal that travels through several kilometers of fiber and amplification stages before regeneration. Examples of signal in the time domain and their associated probability distribution functions (pdfs) are illustrated. For Class I regenerators, the bit error ratio is the same just before (b) and just after (c) regeneration, as quantified by the area under the pdfs common surface (brown-colored). R: Regenerator, A: amplifier.

#72211 - $15.00 USD Received 22 June 2006; revised 27 July 2006; accepted 27 June 2006

2. Concepts of probability distribution function and bit error ratio

Figure 1 shows the schematic of an amplified optical link containing optical regenerators. The bit format used in this system is return to zero (RZ) and consist of optical pulses for logical ones and no power for logical zeros. After a short propagation length (Fig. 1(a)), sampling the signal at the center of each bit to find out whether the bit is a logical one or a logical zero leads to two clearly defined power levels: A relatively high power level for the logical ones and a relatively low power level for the logical zeros. Such a clearly defined, two-level signal can be decoded without any error. As the signal propagates along the system containing cascaded amplifiers, it degrades and become noisy under the influence of beating with amplified spontaneous emission (ASE) (Fig. 1(b)). At this stage, sampling the center of each bit leads to two broadened power distribution corresponding to the logical ones and logical zeros. With sufficient accumulation of ASE noise, the power distribution of logical ones and logical zeros overlap and become hard to distinguish. At this stage, a receiver would recover the signal with a number of errors that depends on the degree of overlap between the two power levels.

Power distributions of the logical ones and logical zeros are well represented by probability distribution functions (pdfs). A pdf quantifies the probability for a given sampled bit to lead to a desired power level. For instance, the probability for a sampling event E that the power level P_E is found between levels a and b is

$$Prob[\, a < P_E < b \,] = \int_a^b pdf(P)\,dP \tag{1}$$

where $pdf(P)$ follows the statistics of the event E, and P represents possible power levels at sampling time. An important characteristic of pdfs is that the complete surface under a pdf, or equivalently the integral over all possible power values, always equals 1. From our previous example, the probability that P_E is comprised between power levels a=0 and b=∞ equals 100% - it is a *certain* event because a power level is a real number that *must* be comprised between 0 and ∞.

Pdfs are indispensable tools to quantitatively describe the power levels of noisy bits in a communication system. As mentioned earlier, when power levels (or pdfs) of logical ones and logical zeros overlap, bit levels become hard to distinguish and errors occur at the receiver. Quantitatively, the BER of a noisy signal is found from the pdf of the logical ones (pdf_1) and the logical zeros (pdf_0) following,

$$BER = \frac{1}{2}\int_0^T pdf_1(P)\,dP + \frac{1}{2}\int_T^\infty pdf_0(P)\,dP \tag{2}$$

where T is a power level that represents the decision threshold. Eq. (2) is valid for a signal that is equally composed of logical ones and logical zeros. The sampled bit which has a power level *above* the decision threshold is interpreted as a *logical one* whereas the sampled bit which has a power level *below* the decision threshold is interpreted as a *logical zero*. An error therefore arises when a bit is so noisy that its power at sampling time is on the wrong side of the decision threshold. The decision threshold must be carefully chosen from pdf_1 and pdf_0 to avoid inducing an artificially high *BER*. The optimal decision threshold which minimizes *BER* is found by differentiating Eq. (2) with respect to T and setting $dBER/dT=0$. This gives $pdf_1(T_O)=pdf_0(T_O)$ as the solution for the optimal decision threshold T_O. The optimum threshold is therefore found at the common power coordinate where $pdf_1(P)$ and $pdf_0(P)$ intersect. As a result, the BER as expressed in Eq. (2) represents the surface integral under the common area of $pdf_1(P)$ and $pdf_0(P)$.

#72211 - $15.00 USD Received 22 June 2006; revised 27 July 2006; accepted 27 June 2006

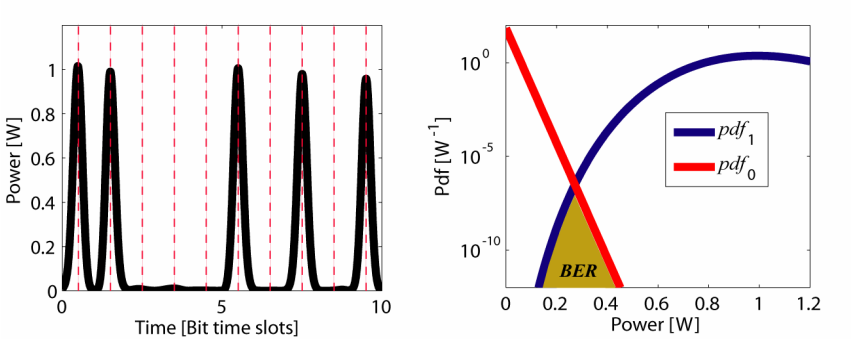

Fig. 2. A sample of 10 bits of a noisy signal (left graph) and the probability distribution functions for the logical ones and logical zeros at sampling time (right graph). The sampling time is represented by the red dotted line. The optimal threshold is T_O=0.269 W, as seen from the crossing point between pdf_1 and pdf_0. The BER of this signal is 4.7×10^{-9} as measured from the common surface under both pdfs (brown-colored).

Figure 2 presents a 10 bits sample of noisy signal (left graph) and the corresponding pdfs for the logical ones and the logical zeros (right graph). The optimal threshold is T_O=0.269 W as found from the crossing point of the two pdfs. For this signal, errors statistically occur at a ratio of BER=4.7×10^{-9}, as can be evaluated from the common surface under pdf_1 and pdf_0.

3. Signal conversion by power transfer functions

In this section we clarify the impact of signal conversion with one or several power transfer functions, with a special emphasis on the associated BER. We show that a first class of regenerators that redistribute the power from a single power transfer function cannot improve the BER of a signal. This class of regenerators is referred to as *Class I* regenerators. In contrast, we show that a second class of regenerators, referred to as *Class II* regenerators, ruled by more than one power transfer function can improve the BER of a signal, if properly engineered.

Before considering the BER after regeneration, it will be useful to define a BER before regeneration (BER_-) such as

$$BER_- = \frac{1}{2}\int_0^{T_{O-}} pdf_{1-}(P_-)dP_- + \frac{1}{2}\int_{T_{O-}}^{\infty} pdf_{0-}(P_-)dP_- . \tag{3}$$

where the – subscript refers to parameters before regeneration. Equation (3) is expressed directly from Eq. (2) taking into consideration an optimal threshold T_{O-} as defined by the crossing point between the two pdfs, or $pdf_{0-}(T_{O-})=pdf_{1-}(T_{O-})$

3.1 Class I Regenerators

We now evaluate the BER of a noisy signal after passing through an optical regenerator that has a single power transfer function, the Class I regenerator. A Class I regenerator converts an input signal (P_-) into an output signal (P_+) by means of a power transfer function,

$$P_+ = f(P_-). \tag{4}$$

The + subscript refers to parameters after regeneration. The power transfer function is considered to increase monotonically (i.e. $f(P_-+dP)\geq f(P_-)$ for all $P_->0$ and $dP>0$) and therefore has an inverse solution $P_-=f^{-1}(P_+)$. From the power transfer function, an input pdf (pdf_-) describing the instantaneous power levels entering the class I regenerator can be converted into an output pdf (pdf_+) directly from [12],

#72211 - $15.00 USD Received 22 June 2006; revised 27 July 2006; accepted 27 June 2006

$$pdf_{+}(P_{+}) = pdf_{-}\left(f^{-1}(P_{+})\right) \left|\frac{df^{-1}(P_{+})}{dP_{+}}\right| \equiv \Im\left[pdf_{-}(P_{-})\right] \tag{5}$$

where $\Im$ is a pdf transformation operator that converts pdf_{-} into pdf_{+}. The output BER calculation for a Class I regenerator, which we label as BER^{I}_{+}, is obtained by transforming the input pdfs of the logical ones and the logical zeros with the pdf transformation operator $\Im$, using Eqs. (2) and (5)

$$BER^{I}{}_{+} = \frac{1}{2}\int_{0}^{T_{+}} pdf_{1+}(P_{+})dP_{+} + \frac{1}{2}\int_{T_{+}}^{\infty} pdf_{0+}(P_{+})dP_{+} \,. \tag{6}$$

The optimal threshold is found from $dBER^{I}_{+}/dP_{+}=0$ and leads to $pdf_{1+}(T_{O+})=pdf_{0+}(T_{O+})$. We rewrite Eq. (6) in consequence,

$$BER^{I}{}_{+} = \frac{1}{2}\int_{0}^{T_{O+}} pdf_{1+}(P_{+})dP_{+} + \frac{1}{2}\int_{T_{O+}}^{\infty} pdf_{0+}(P_{+})dP_{+} \,. \tag{7}$$

We now want to link pdf_{1+} and pdf_{0+} to their pdfs before conversion. Equation (5) is used for this purpose

$$BER^{I}{}_{+} = \frac{1}{2}\int_{0}^{T_{O+}} \Im\left[pdf_{1-}(P_{-})\right]dP_{+} + \frac{1}{2}\int_{T_{O+}}^{\infty} \Im\left[pdf_{0-}(P_{-})\right]dP_{+} \,. \tag{8}$$

$$BER^{I}{}_{+} = \frac{1}{2}\int_{0}^{T_{O+}} \Im\left[pdf_{1-}\left(f^{-1}[P_{+}]\right)\right]dP_{+} + \frac{1}{2}\int_{T_{O+}}^{\infty} \Im\left[pdf_{0-}\left(f^{-1}[P_{+}]\right)\right]dP_{+} \,. \tag{9}$$

The power transfer function has performed a change of variables on both pdfs of Eq. (7). However, a variable change within an integral does not change its result[*]. As a consequence, we can reapply a change of variables using the inverse $\Im$ operator ($\Im^{-1}$) on Eq. (9) to convert back the expression of BER^{I}_{+} in the P_{-} space. We then find,

$$BER^{I}{}_{+} = \frac{1}{2}\int_{0}^{f^{-1}(T_{O+})} \Im^{-1}\left\{\Im\left[pdf_{1-}\left(f\left[f^{-1}\{P_{-}\}\right]\right)\right]\right\}dP_{-} + \frac{1}{2}\int_{f^{-1}(T_{O+})}^{\infty} \Im^{-1}\left\{\Im\left[pdf_{0-}\left(f\left[f^{-1}\{P_{-}\}\right]\right)\right]\right\}dP_{-} \tag{10}$$

$$\begin{aligned} BER^{I}{}_{+} &= \frac{1}{2}\int_{0}^{T_{O-}} pdf_{1-}(P_{-})dP_{-} + \frac{1}{2}\int_{T_{O-}}^{\infty} pdf_{0-}(P_{-})dP_{-} \\ &= BER^{I}{}_{-} \end{aligned} \tag{11}$$

[*] As a recall from variable changes into integrals, one can convince himself by taking an example like $\int_{a}^{b} x^{2}dx = \frac{b^{3}-a^{3}}{3}$ and prove that changing the variables (e.g., $x=y^{1/2}$, $dx=dy/2y^{1/2}$, upper bound x=b changed for $y=b^{2}$ and lower bound $x=a$ changed for $y=a^{2}$) does not affect the final result.

#72211 - $15.00 USD Received 22 June 2006; revised 27 July 2006; accepted 27 June 2006

No BER change is achieved when the logical ones and logical zeros are converted by the same monotonic power transfer function. This result directly applies to any optical regenerator of Class I. Therefore, a Class I regenerator do not improve the BER of the signal passing through it. Following a more complex reasoning, it is found that when the power transfer function is non-monotonic, i.e., when $f(P_+)$ contains more than one local maximum and/or discontinuities- then $BER^I_+ \geq BER^I_-$. Therefore, *the BER after conversion with a single power transfer function is worse (higher) or at most equal to the BER before conversion, independently of the shape of the power transfer function.* We keep this last result as a general result for both monotonic and non-monotonic power transfer functions of Class I.

Although they do not improve the BER, the power transfer function of Class I regenerators acts on the signal by flattening the power fluctuations on the logical ones and on the logical zeros. This has the effect of decreasing the noise buildup from subsequent amplification stages. With Class I regenerators, the BER still increases along the transmission path containing amplifiers and regenerators, but not as dramatically as if there was no regenerator. This justifies the use of Class I regenerators in systems even if they do not improve the BER. To our knowledge, every optical regenerator that has been proposed to date is a Class I regenerator, the only exceptions to this rule are the 2R regenerator based on spectral broadening followed by filtering [9]-[11] and the 3R regenerator architecture based on spectral shift and filtering (discussed in this paper).

Figure 3 presents the signal exemplified in Fig. 2 before and after processing by a Class I regenerator. The regenerator has a single power transfer function (left graph) and we show the pdfs before and after conversion by the power transfer function (right graph). The pdfs after conversion are found from Eq. (5) and superimposed on the pdfs before conversion. This example shows that although the pdfs have changed shape and crossing point (T_O=0.269 W, T_+=0.171 W), the BER remains the same at BER=4.7×10^{-9} in both cases.

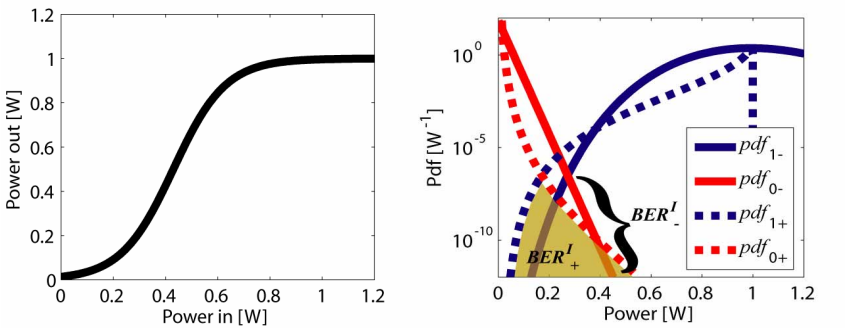

Fig. 3. Example of Class I power transfer function (left graph) and pdfs before and after conversion with the power transfer function (right graph). The profile of the pdfs and the optimal threshold have been modified in the conversion but the corresponding bit error ratio remains 4.7×10^{-9} in both cases.

3.2 Class II Regenerators

From a system viewpoint, it is highly desirable to periodically reduce the BER of a noisy signal in an optical link, not just prevent a noise buildup. Regenerators that operate with different power transfer functions on the logical ones and on the logical zeros –Class II regenerators- can do this. To calculate the output BER of a Class II regenerator (BER^{II}_+), with distinct power transfer functions for logical ones and logical zeros, Eq. (5) is used with both pdf_1- and pdf_0- converted individually following their pdf transformation operator, that is $\Im_1$ and $\Im_0$ respectively,

#72211 - $15.00 USD Received 22 June 2006; revised 27 July 2006; accepted 27 June 2006

$$BER^{II}{}_{+} = \frac{1}{2}\int_{0}^{T_{+}} pdf_{1+}(P_{+})dP_{+} + \frac{1}{2}\int_{T_{+}}^{\infty} pdf_{0+}(P_{+})dP_{+} . \tag{12}$$

The optimal threshold is found from $dBER^{II}{}_{+}/dP_{+}=0$ and leads to $pdf_{1+}(T_{O+})=pdf_{0+}(T_{O+})$. We rewrite Eq. (12) in consequence,

$$BER^{II}{}_{+} = \frac{1}{2}\int_{0}^{T_{O+}} pdf_{1+}(P_{+})dP_{+} + \frac{1}{2}\int_{T_{O+}}^{\infty} pdf_{0+}(P_{+})dP_{+} . \tag{13}$$

We now link pdf_{1+} and pdf_{0+} to their pdfs before conversion using Eq. (5),

$$BER^{II}{}_{+} = \frac{1}{2}\int_{0}^{T_{O+}} \Im_1[pdf_{1-}(P_{-})]dP_{+} + \frac{1}{2}\int_{T_{O+}}^{\infty} \Im_0[pdf_{0-}(P_{-})]dP_{+} , \tag{14}$$

$$BER^{II}{}_{+} = \frac{1}{2}\int_{0}^{T_{O+}} \Im_1\left[pdf_{1-}\left(f_1^{-1}[P_{+}]\right)\right]dP_{+} + \frac{1}{2}\int_{T_{O+}}^{\infty} \Im_0\left[pdf_{0-}\left(f_0^{-1}[P_{+}]\right)\right]dP_{+} . \tag{15}$$

To facilitate the comparison with the BER before regeneration, $BER^{II}{}_{+}$ is converted into the P_{-} space using the inverted $\Im_1$ operator (i.e., $\Im_1^{-1}$) in both integrands of Eq. (15). This conversion does not change the result of the integration and gives

$$BER^{II}{}_{+} = \frac{1}{2}\int_{0}^{T_{O+}} pdf_{1-}\left(f_1^{-1}[P_{+}]\right)dP_{+} + \frac{1}{2}\int_{T_{O+}}^{\infty} \Im_1^{-1}\left\{\Im_0\left[pdf_{0-}\left(f_0^{-1}[P_{+}]\right)\right]\right\}dP_{+} . \tag{16}$$

$$BER^{II}{}_{+} = \frac{1}{2}\int_{0}^{f_1^{-1}(T_{O+})} pdf_{1-}(P_{-})dP_{-} + \frac{1}{2}\int_{f_1^{-1}(T_{O+})}^{\infty} \Im_1^{-1}\left\{\Im_0\left[pdf_{0-}\left(f_0^{-1}[f_1\{P_{-}\}]\right)\right]\right\}dP_{-} . \tag{17}$$

The inverse pdf transformation operator $\Im_1^{-1}$ over (15) leaves Eq. (17) with a first integrand that contains only $\Im_1^{-1}[\Im_1(pdf_{1-})]=pdf_{1-}$ and therefore resembles the first integrand in Eq. (3). In contrast, the second integrand of Eq. (17) comprises a double transformation of pdf_{0-} that does not equals the second integrand of Eq. (3) unless $\Im_0=\Im_1$. As a result, a Class II regenerator with non-similar power transfer functions affecting independently logical ones and logical zeros lead to $BER^{II}{}_{+}\neq BER^{II}{}_{-}$. We conclude that when the pdfs expressing logical ones and logical zeros are converted with distinct power transfer functions, the resulting BER is whether increased or reduced depending on the power transfer functions involved.

In order to get an improvement of the BER after conversion, or

$$BER^{II}{}_{-} > BER^{II}{}_{+} , \tag{18}$$

we introduce Eqs. (17) and (3) into Eq. (18) and take the limit where f_1 and f_0 are just slightly different. In this limit, just the second integrals of Eqs. (17) and (3) need to be taken into consideration since $f_1^{-1}(T_{O+})\sim T_{O-}$ and the first integrals cancel each other. This leads to the condition

$$\int_{T_{O-}}^{\infty} pdf_{0-}(P_{-})dP_{-} > \int_{T_{O-}}^{\infty} \Im_1^{-1}\left\{\Im_0\left[pdf_{0-}\left(f_0^{-1}[f_1\{P_{-}\}]\right)\right]\right\}dP_{-} . \tag{19}$$

#72211 - $15.00 USD Received 22 June 2006; revised 27 July 2006; accepted 27 June 2006

One solution of Eq. (19) is that $f_1(P_-)>f_0(P_-)$ for all input power values $P_->0$ and independently of pdf_{0-}.

Figure 4 shows the example of a Class II regenerator with different power transfer functions that affect the logical ones and the logical zeros independently and follow$f_1(P_-)>f_0(P_-)$ (upper left graph). A pdf conversion using these power transfer functions leads to pdfs with different shapes and thresholds (T_{O-}=0.269 W, T_{O+}=0.126 W), but also leads to a BER improvement from $BER^{II}_-=4.7\times10^{-9}$ before conversion to $BER^{II}_+=3.7\times10^{-10}$ after conversion (upper right graph). An equivalent way to evaluate the BER is to compare pdf_{1-} with both pdf_{0-} and its double converted operation $\Im_1^{-1}(\Im_0(pdf_{0-}))$ (lower graph). The resulting graph shows a clear BER improvement, or surface area reduction, from $\Im_1^{-1}(\Im_0(pdf_{0-}))$ being at lower values than pdf_{0-}. Once again, the BER is improved from $BER^{II}_-=4.7\times10^{-9}$ before conversion to $BER^{II}_+=3.7\times10^{-10}$ after conversion.

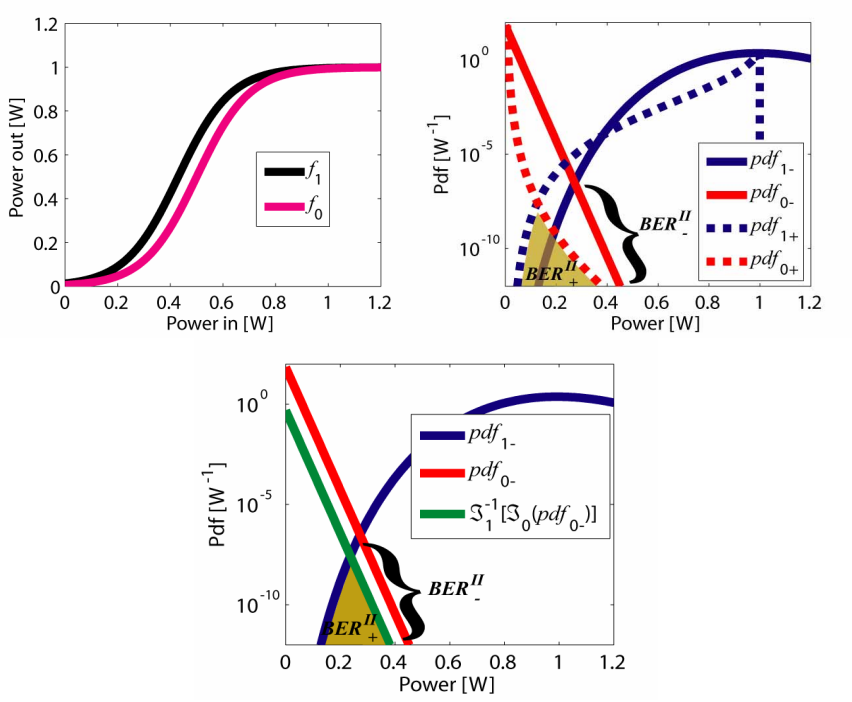

Fig. 4. Distinct power transfer functions for the logical ones and the logical zeros (upper left graph) and pdfs before and after conversion with the power transfer functions (PTFs) (upper right graph). The pdfs before conversion provide $BER^{II}_-=4.7\times10^{-9}$ whereas the pdfs after conversion provide $BER^{II}_+=3.7\times10^{-10}$. The origins of this BER improvement come from the power transfer function of the logical ones which is closer to the upper power level, with respect to the power transfer function of the logical zeros. Plot of pdf_0, pdf_1 and $\Im_1^{-1}(\Im_0(pdf_{0-}))$ providing a clear comparison between BER before and BER after conversion with distinct power transfer functions (lower graph). The BER after regeneration is evaluated from the common surface under $\Im_1^{-1}(\Im_0(pdf_{0-}))$ and pdf_1, $BER^{II}_+=3.7\times10^{-10}$.

Figure 5 presents the example of a Class II regenerator that will be important in the remaining of the text. The power transfer functions of this regenerator lead to bit inversion, that is, a logical one is converted into a logical zero and vice-versa (upper left graph). In this case, the requirements for BER improvement from Eq. (19) is that $f_1(P_-)<f_0(P_-)$ for all input power values $P_->0$ and independently of pdf_{0-}. A pdf conversion using these power transfer functions leads to pdfs with different shapes and thresholds (T_{O-}=0.269 W, T_{O+}=0.874 W), but also a BER improvement from $BER^{II}_-=4.7\times10^{-9}$ before conversion to $BER^{II}_+=3.7\times10^{-10}$ after conversion (upper right graph). Using the comparison of pdf_1 with both pdf_0 and its double

#72211 - $15.00 USD Received 22 June 2006; revised 27 July 2006; accepted 27 June 2006

converted operation $\Im_0^{-1}(\Im_0(pdf_{0-}))$ provides a clear view of the BER improvement (lower graph). The BER improvement between the example of Fig. 4 and this example are identical because the same power transfer functions have been used, with the only difference that they have been flipped symmetrically around the horizontal axis to invert the bits in this example.

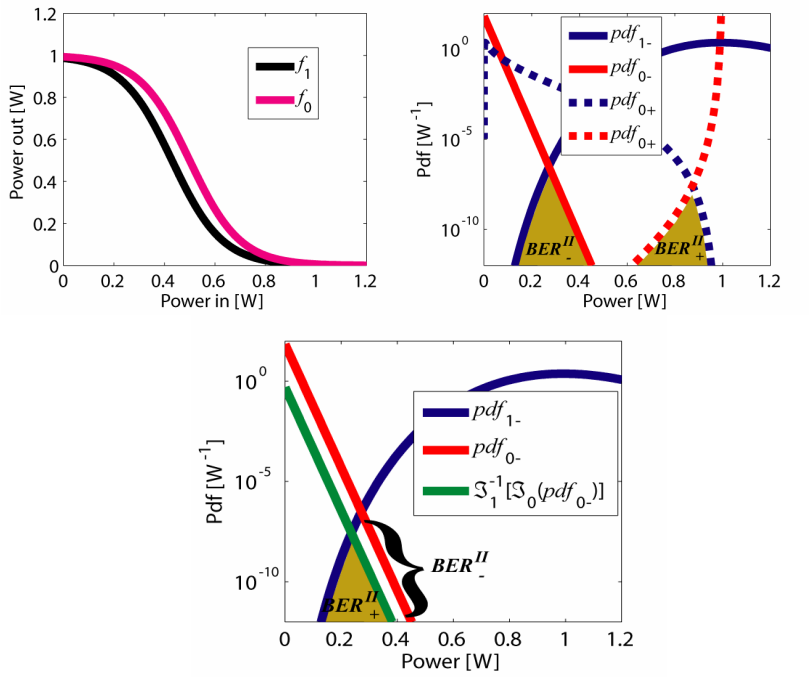

Fig. 5. Distinct power transfer functions (PTFs) for the logical ones and the logical zeros (upper left graph) leading to bit inversion, and pdfs before and after conversion with the power transfer functions (upper right graph). The pdfs before conversion provide $BER^{II}_-=4.7\times10^{-9}$ whereas the pdfs after conversion provide $BER^{II}_+=3.7\times10^{-10}$. Plot of pdf_0, pdf_1 and $\Im_0^{-1}(\Im_0(pdf_{0-}))$ providing a graphic comparison between BER before and BER after conversion with distinct power transfer functions (lower graph). The BER after regeneration is evaluated from the common surface under $\Im_0^{-1}(\Im_0(pdf_{0-}))$ and pdf_1, $BER^{II}_+=3.7\times10^{-10}$.

In the context of an optical signal with an RZ modulation format, power transfer functions that are different for logical ones and logical zeros mean different power transfer functions for noisy pulses (pulsed logical ones + ASE noise) and ASE noise alone. As a result, an optical regenerator that discriminates noisy pulses from noise alone, by affecting them with different power transfer functions, is a Class II regenerator, and can therefore improve the BER of an RZ signal, if properly engineered. The next section discusses this case with more details.

4. Principle and operation of the 3R regenerator with BER improvement

The architecture and principle of the 3R regenerator with BER improvement are illustrated in Fig. 6. The regenerator architecture was proposed by Suzuki *et al*. [8] and consists of an optical clock source, an erbium-doped fiber amplifier (EDFA), a highly nonlinear fiber (HNLF), and a band-pass filter (BPF). The clock is generated from a clock-recovery circuit and produces pulses of shorter duration than the pulses to regenerate. The repetition rate of the clock can be chosen equal to the signal data rate when regeneration is desired. Also, the repetition rate of the clock can be smaller than the signal data rate when regeneration and demultiplexing are desired. The signal bits at wavelength λs and the clock pulses at wavelength λc spatially overlap as they enter the HNLF (Fig. 6(b)). The clock spectrum

#72211 - $15.00 USD Received 22 June 2006; revised 27 July 2006; accepted 27 June 2006

experiences a cross-phase modulation (XPM)-induced frequency shift $\delta\omega_{XPM}$ proportional to the slope of the superimposed signal,

$$\delta\omega_{XPM}(t) = -2\gamma L_{Eff}\frac{dP(t)}{dt} \tag{20}$$

where γ is the fiber nonlinearity, L_{Eff} is the effective fiber length, $P(t)$ is the input signal, and t is time. The output filter BPF_2 filters out the spectral components that have been shifted by XPM and keeps the original frequency components at wavelength λc. Take note that this regeneration architecture is inverting the bits, i.e., logical ones are transformed into logical zeros and vice-versa. A non-inverting mode can also be achieved by offsetting the center frequency of BPF_2 away from the original clock wavelength, in order to transmit only XPM generated frequencies. In both case, the power transferred from the input to the output of the regenerator depends on $\delta\omega_{XPM}$ and hence the power transfer function depends on the temporal characteristics – namely the derivative - of the instantaneous input power, as expressed in Eq. (20). As a consequence, this 3R regenerator has the interesting capability to discriminates an abruptly varying signal from a slowly varying signal. This is in contrast with conventional regeneration schemes, or Class I regenerators, into which the power transfer function converts solely the instantaneous input power as expressed in Eq. (4), without regard to its derivatives. The capability of discriminating the slope (and therefore the width) of a pulse is a first step leading to the discrimination between noisy pulses and ASE noise alone. The second and last step to achieve signal discrimination is provided from the temporal shape of noisy pulses and ASE noise alone, as explained below.

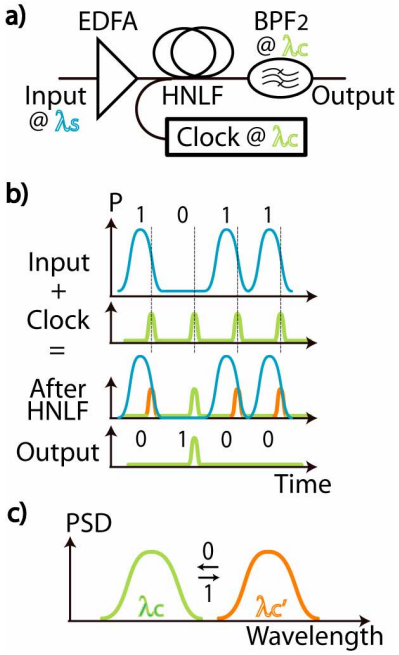

Fig. 6. (a) Schematic of the 3R regenerator based on XPM-induced spectral shift followed by filtering. (b) The low power clock pulses are overlapping with the edge of the high power signal pulses, which induce a spectral shift on the clock. At the output of the regenerator, data have been imprinted at the clock wavelength, and inverted. (c) The clock spectrum is composed of two lobes after XPM (i.e. after HNLF). One lobe at λc is identical to the clock spectrum before XPM and a second lobe at λc' is a spectrally shifted replica of the clock spectrum. The first lobe is formed by input logical zeros whereas the second lobe is formed by input logical ones. λs/c: Wavelength for signal/clock. P: Power. PSD: Power spectral density.

#72211 - $15.00 USD Received 22 June 2006; revised 27 July 2006; accepted 27 June 2006

In an optical network, where ASE noise accumulates as a result of cascaded amplifiers, an RZ logical one consists of a pulse interfering with ASE noise, whereas a logical zero is represented exclusively by ASE noise, as depicted in Fig. 7. At the regenerator input, the spectra for the pulse and the ASE noise are considered identically Gaussian. This profile results from signal and ASE passing through multiplexing/demultiplexing filters distributed in the network before regeneration. The relative spectral amplitude or equivalently the average power ratio between pulse and ASE are governed by the optical signal to noise ratio (OSNR) as evaluated in a spectral bandwidth of 0.1 nm. In the time domain, the logical ones consist of noisy pulses with random amplitude jitter depending on the OSNR (Fig. 7(b)-(c)). Although the peak power of the noisy logical ones varies from one pulse to the other as a result of beating with noise, the pulse width and pulse shape are mainly conserved when OSNR>15 dB. Figure 7(d) shows the pulse width fluctuation between noisy logical ones of identical OSNR, expressed as the ratio between the standard deviation and the mean pulse width, as a function of OSNR. For OSNR>15 dB, the pulse width variation for the noisy logical ones is below 4%. Contrasting with the relatively stable pulse width of the noisy logical ones, the logical zeros are composed only of ASE noise, and in the time domain they appear as a collection of pulses with random width and amplitude, as depicted in Fig. 7(a). The statistical distribution of pulse width is limited on the short timescale side by the Fourier transform of the noise spectrum, but is unlimited on the long timescale side. As a consequence, ASE noise appears as a collection of pulses of width equal or larger than the logical ones. This fundamental property that distinguish nearly transform-limited logical ones from ASE noise, combined with the pulsewidth discrimination of the 3R regenerator, together enable BER improvement.

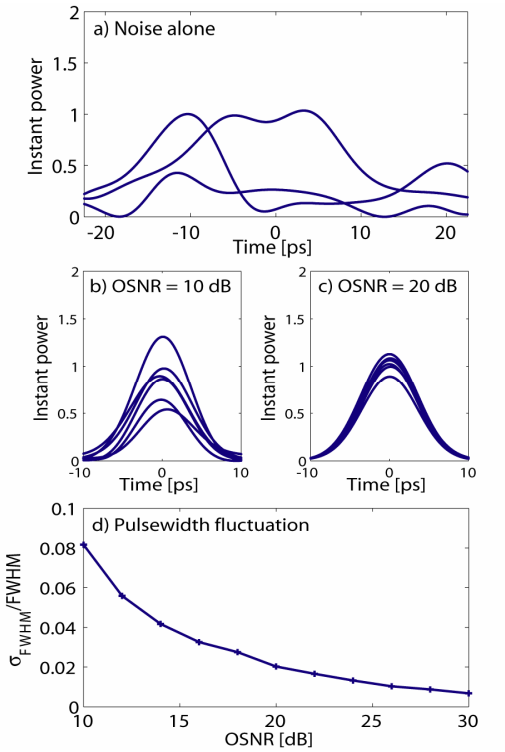

Fig. 7. (a) Temporal waveforms for ASE noise alone and (b-c) noisy pulses. (b) Pulses with OSNR=10 dB and in (c), pulses with OSNR=20 dB. (d) Pulsewidth fluctuation as a function of OSNR. Calculated from 100 noisy pulses at every OSNR value. The pulsewidth fluctuation is expressed as the standard deviation (σ_{FWHM}) divided by the average pulsewidth (FWHM). The spectra of ASE noise and pulses are identically Gaussian with 53 GHz spectral width in all simulations of this figure.

#72211 - $15.00 USD Received 22 June 2006; revised 27 July 2006; accepted 27 June 2006

5. Experimental demonstration of BER Improvement

The basic 3R functionality of the regenerator architecture based on the principle of spectral shift followed by filtering has already been demonstrated by Suzuki *et al*. [8]. We therefore focus on the demonstration that this 3R regenerator discriminates pulses of different widths and that it can improve the BER. Figure 8(a) shows the setup used to demonstrate that the 3R regenerator discriminates pulses of different widths. For this purpose, the output versus input peak power (i.e. power transfer function) is measured for pulses of different duration: 8 ps, 16 ps, and ∞ ps (or continuous wave light). Figure 8(b) shows the setup used to demonstrate BER improvement by the regenerator. For this second experiment, a pattern generator sends a pseudo-random bit sequence (PRBS) of 2^{23}-1 bits at a rate of 40 Gb/s. The bits are transformed by cascaded modulators into 8 ps pulses at a wavelength of 1534.25 nm and with a bandwidth of 0.5 nm, respectively. The pulsed signal and ASE noise from an EDFA are combined to a desired OSNR using a variable attenuator VA_1 and a 3 dB coupler. The ASE noise source and the pulsed signal are spectrally filtered in an identical fashion using a band-pass filter of 0.5 nm. The 3R architecture follows the schematic of Fig. 6(a) with the following parameters: the clock source sends pulses of 4 ps at a wavelength of 1558.0 nm, the HNLF has a length of 850 m and a nonlinearity γ=20 $W^{-1}Km^{-1}$, the bandpass filter BPF_2 has a width of 0.5 nm and is centered at 1558.0 nm, the amplifier boosts the noisy pulses up to a peak power level sufficient (500 mW) to induce XPM on the clock. The regenerator is followed by a variable attenuator VA_2 that ensures that the maximum peak optical power sent to the photodiode is maintained at a constant level of 2 mW. At this relatively high optical power level, shot noise and thermal noise have a negligible contribution over the total noise measured. For instance, the measured BER<<1×10^{-13} (no errors) when measuring the 2 mW signal free from ASE at the photodiode input. In contrast, when ASE noise is superimposed to the signal, we obtain BER=1×10^{-10} to 1×10^{-2} depending on the OSNR adjustment. Signal-spontaneous beat noise is therefore the most prominent source of noise when ASE noise is present. The 2 mW optical signal converts into a 285 mV electrical signal at the photodiode output. A BER tester receives the noisy electrical signal with or without the 3R regenerator in the measurement setup and counts the number of errors for various levels of OSNR.

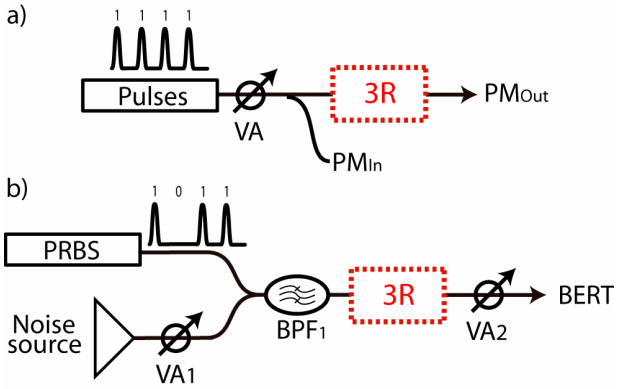

Fig. 8. (a) Experimental setup for the power transfer function measurement. (b) Setup to demonstrate BER improvement. The 3R regenerator is identical to the one shown in Fig. 6. a. VA: Variable attenuator. PM_{In}/PM_{Out}: Power meter at the input/output of the O3R. BPF: Band-pass filter. PRBS: Pseudo random bit sequence. BERT: Bit error ratio tester.

The measured power transfer functions are shown in Fig. 9(a). For a given input peak power, different pulse widths lead to different XPM spectral shift and therefore different power transmission through BPF_2. The extreme case of a continuous wave signal, with no

#72211 - $15.00 USD Received 22 June 2006; revised 27 July 2006; accepted 27 June 2006

power slope, does not induce any XPM and the clock is therefore completely transmitted through BPF_2. The situation is different for 8 ps and 16 ps pulses where the amount of power transmitted through BPF_2 depends both on the peak pulse power and width of the input signal. The regenerator clearly discriminates pulses of different widths, and therefore discriminate logical ones (8 ps pulses, synchronized with the clock) from logical zeros (>8 ps pulses, asynchronized with respect with the clock). As shown in Fig. 4 and Fig. 5, even a small difference between power transfer function profiles associated to logical ones and logical zeros is expected to significantly affect the BER. The only difference between examples of Fig. 4, Fig. 5 and the actual demonstration is that in this case, logical zeros follow more than one power transfer function, depending on the many possible noise shape that superimpose with the clock. Of all the possible power transfer function, the noise shape always have a width larger than 8 ps and will therefore follow a power transfer function having $f_1(P_-)<f_0(P_-)$ for every P_-. Taking into consideration that the 3R regenerator is inverting the bits and that we experimentally measured that $f_1(P_-)<f_0(P_-)$ for every P_- ensures a BER improvement.

Figure 9(b) shows the BER of the noisy signal before and after regeneration, for various OSNR levels. The result shows a BER improvement from $BER_-=3\times10^{-6}$ without regenerator to $BER_+=2\times10^{-10}$ with regenerator. This represents nearly four orders of magnitude in BER improvement at an OSNR=15 dB. Alternatively, the regenerator provides an OSNR margin of 4 dB at a BER of 10^{-10}. To test the reproducibility, the experiment was repeated a few times (twice on Fig. 9(b)) and gave identical results. We believe that further improvement of the BER is possible by optimizing the regenerator parameters such as the length of nonlinear medium, the nominal peak power in the regenerator, and the spectral shift of BPF_2.

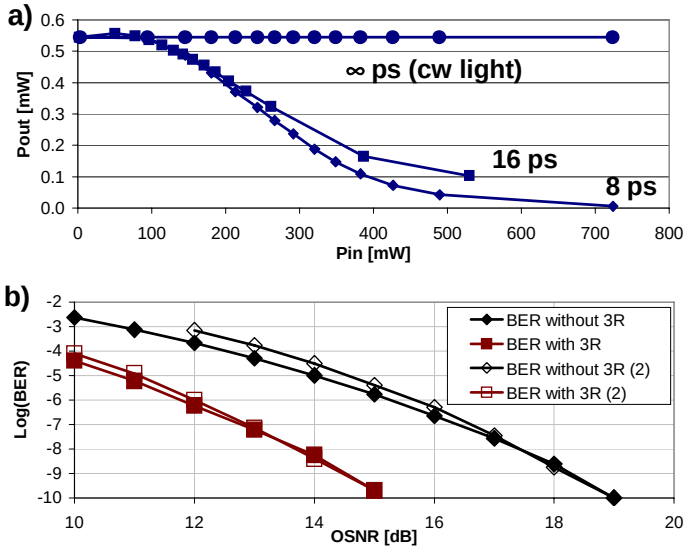

Fig. 9. (a), power transfer functions for 8 ps pulses, 16 ps pulses, and continuous wave (cw) light. The input and output powers, Pin and Pout, are expressed in terms of peak power. (b) BER with and without the regenerator as a function of OSNR and constant received power. The 3R regenerator improves the BER for constant OSNR or equivalently, the 3R regenerator increases the OSNR margin for a given BER.

6. Conclusion

We have shown that a 3R regenerator based on the principle of XPM spectral shift followed by filtering have the powerful capability to improve the BER of a signal added with spontaneous emission noise. The origin of this improvement arises from the capacity of the regenerator to discriminate pulses of different widths by assigning them different power

#72211 - $15.00 USD Received 22 June 2006; revised 27 July 2006; accepted 27 June 2006

transfer functions. As a result, the regenerator discriminates the logical ones from the logical zeros in a noisy signal. We have provided the theoretical basis that supports these conclusions. We presented Class I regenerators that are characterized by a single power transfer function and we have shown that they cannot improve the BER of a noisy signal. In contrast, Class II regenerators are characterized by distinct power transfer functions associated to the logical ones and logical zeros of a noisy signal and only this class of regenerator can improve the BER. We experimentally showed that the 3R regenerator discriminates pulses of different widths by assigning them different power transfer functions. Finally, the BER of a noisy signal was improved by four orders of magnitude by passing through this regenerator. It is expected that further BER improvement would be achieved with a proper optimization of the regenerator parameters. This architecture is the first known to simultaneously enable BER improvement and 3R operation, and is believed to provide an outstanding advantage over standard, non BER improving, regeneration architectures.

Acknowledgments

This work was produced with the assistance of the Natural Science and Engineering Research Council of Canada (NSERC) and the Australian Research Council under the ARC Centres of Excellence program.

#72211 - $15.00 USD Received 22 June 2006; revised 27 July 2006; accepted 27 June 2006